

Theoretical prediction of maximum capacity of C₈₀ and Si₈₀ fullerenes for noble gas storage



Zabiollah Mahdavifar*

Computational Chemistry Group, Department of Chemistry, Faculty of Science, Shahid Chamran University, Ahvaz, Iran

ARTICLE INFO

Article history:

Accepted 25 August 2014

Available online 6 September 2014

Keywords:

C₈₀ and Si₈₀ fullerenes

Noble gas

Encapsulation

DFT calculations

New molecular phenomenon

ABSTRACT

In this paper, we try to demonstrate that how many helium, neon and argon atoms can be trapped into fullerene cages until the pressure becomes large enough to break the C₈₀ and Si₈₀ frameworks. The maximum number of helium, neon and argon atoms which can be encapsulated into C₈₀ fullerene, is found with 46, 24 and 10 atoms respectively. Having investigated the mechanism of C₈₀ opening, we found that if the number of helium and argon atoms reaches to 50 and 12 respectively, the C–C bonds of C₈₀ are broken and the gas molecules escape from the fullerene cage. The final optimization geometries of latter complexes are similar to the shopping cart. Therefore, this appearance is named as molecular cart. Moreover, the maximum capacity of Si₈₀ fullerene for encapsulated noble gas atoms is found 95, 56 and 22 for helium, neon and argon atoms correspondingly. It is worth highlighting that the new phenomenon of trapping argon atoms into Si₈₀ cage is observed, when a Si atom randomly added to the center of Ar₁₉@Si₈₀ structures. In this case, the Si–Si bonds of Si₈₀ are broken and two argon atoms will escape from the cage. After that, the framework rebuilds its structure like the initial one. This phenomenon is introduced as molecular cesarean section. The estimated internal pressure of Ng atoms trapped into the fullerene cages is also investigated. Results show that the maximum calculated internal pressure is related to He₄₆@C₈₀ and He₉₅@Si₈₀ structures with 212.3 and 144.1 GPa respectively.

© 2014 Elsevier Inc. All rights reserved.

1. Introduction

It is well-known that the surprise molecule in the past decade was C₆₀ fullerene. One of the most exciting features of C₆₀ and higher fullerenes is that their carbon cages have inner cavities large enough to encapsulate atoms or even small molecules. Since fullerenes were prepared in 1985 [1] various methods have been devised to put atoms and small molecules inside their hollow cages. It should be mentioned that the first endohedral fullerene was synthesized in 1985 by Smalley, Curl, Kroto and coworkers [2]. Endohedral fullerenes have been formed with lanthanide or alkaline earth metals as charge transfer [3–7] and with noble gases [8–10]. Several years ago Saunders et al. discovered that the C₆₀ molecule could encapsulate the noble gas atoms and other small molecules by heating the fullerene in the presence of the gas for 8 h at 600 °C at a pressure of 3000 atm [11–13]. The higher endohedral fullerenes are also investigated. In 1991 Alvarez et al. [14] succeeded for the first time to encapsulate two La metal atoms into the C₈₀ to form La₂@C₈₀ complex. Additionally, Akasaka et al. [15]

reported on a circular motion of the two lanthanum atoms inside C₈₀. It has to be highlighted that the physical properties of the endohedral metal fullerenes depend upon the particular encapsulated metal. When electropositive metal atoms are encapsulated inside carbon cage, electrons are transferred from the metal to the cage, so that an electronic structure, M⁺(C_{2n})[−] results [16–18]. If the radioactive metals are encapsulated into the fullerene cage, the endohedral metal fullerene may be useful as imaging agents and in nuclear medicine [19,20].

Noble gas atoms can be inserted into the fullerene cages in order to form stable compounds by heating the fullerenes in the presence of the gas at high pressure [21]. The first noble gas (Ng) endohedral fullerenes were synthesized through collision experiments by Schwarz and coworkers [22]. Also, the C₆₀ molecule is large enough to enclose other gas molecules [23]. In the case of C₆₀, Tropin et al. [24] described the kinetics of fullerene cluster growth in C₆₀ solutions in N-methyl-2-pyrrolidone (NMP). Recently, it has been experimentally demonstrated that one noble gas atom can be encapsulated inside fullerenes for whole series up to Xe [12,13]. Also, experimental results indicate that two helium and neon gas atoms can be trapped inside fullerenes [25]. Moreover, Krapp and Frenking [26] reported that all Ng₂@C₆₀ compounds are thermodynamically unstable with respect to the loss of noble gas atoms. In

* Tel.: +98 916 3015227; fax: +98 611 3331042.

E-mail addresses: z.mahdavifar@scu.ac.ir, zb.nojini@scu.ac.ir

addition, Tonner et al. [27] using theoretical calculations indicating that how many noble gases could be placed in the C₆₀ fullerene. They found up to 40 He, 17 Ne, 7 Ar, 6 Kr and 6 Xe atoms can be inserted into the C₆₀ fullerene. Furthermore, in 1998 Saunders et al. [21] reported the two helium atoms trapped inside of the C₇₀ fullerene cage. Theoretical barriers for helium to penetrate the benzene rings of the fullerene molecule have been calculated to be greater than 200 kcal/mol⁻¹ [28]. These gases can then be released by breaking of one or more carbon bonds or a “window mechanism” during step heating under vacuum [29,30]. These results convincingly showed that the helium is trapped inside of the fullerene molecule (He@C₆₀) and there is no exchange with the atmosphere [31].

It is worthy of note that researchers have been working to find some stable carbon-like silicon fullerenes. Silicon and carbon belong to the same group, group IV, of the periodic table, and they have similar valence electron configurations. This raises the question of whether carbon can be substituted by silicon in its nanostructures. On the other hand, silicon has a larger atomic radius and lower electronegativity than carbon and due to the lack of sp² bonding in silicon, and pure hollow silicon cages are known to be unstable [32]. Recently, much attention has been focused on how to stabilize silicon fullerenes [33–36] in this regard, Hiura et al. [37] reported the formation of series of metal-containing hydrogenated silicon clusters using an ion trap and indicated that the metal atom was endohedral and it stabilized the Si polyhedral cage [38]. Accordingly, several considerable experimental researches [37,39,40] have reported the formation of a series of metal-containing silicon clusters. If an appropriate metal atom is elected, the properties of Si_n clusters can be tuned. On the theoretical view, there have been many ab-initio and Density Functional Theory (DFT) investigations of silicon clusters with 8–20 atoms encapsulating 3d, 4d and 5d metal atoms [41]. Calculations based on the DFT have suggested that smaller magic clusters such as Al₁₂X (X=Si, Ge, Sn, Pb) and Ba@Si₂₀ as endohedral units might possibly stabilize Si₆₀ into a cage structure [38].

The current research maintains the use of DFT in order to investigate how many He, Ne and Ar noble gas atoms can be trapped inside C₈₀ and Si₈₀ fullerenes until the pressure breaks the fullerene nanocage. Furthermore, the mechanism of fullerene nanocage opening is also considered. In addition, the formation energy, optimized geometry, physical and electronic properties of endohedral C₈₀ and Si₈₀ fullerenes versus the number of encapsulated gas atoms are also investigated.

2. Computational details

In the course of the geometry optimizations and the total energy calculations, the generalized gradient approximations (GGA) were chosen in order to describe the exchange and correlation potential. It has to be stated that the employed parameterization was that of Perdew, Burke, and Ernzerhofer (PBE) [42]. A double-zeta polarized (DZP) basis set [43] was chosen to carry out the electronic structure calculation. It is vital to note that geometry optimizations were performed by the SIESTA (Spanish Initiative for Electronic Simulations with Thousands of Atoms) code [44–46] without any symmetry restrictions. In addition, all the atomic coordinates relaxed together with the super cells using a conjugate gradient (CG) algorithm, until each component of the stress tensor was below 1.0 GPa. An energy cutoff of 150 Ry is used for the plane wave expansion of the electronic wave function. In our SIESTA calculations, a super cell model is employed such that the fullerene was put in a large computational box with sufficient vacuum space surrounding the fullerene that prevents interaction between periodic images. Special k points were generated with the 1 × 1 × 1 grid based on the

Monkhorst-Pack scheme. In each case, all the atoms in the unit cell were relaxed until the residual forces converged to below 0.01 eV Å⁻¹. Furthermore, Natural Bond Orbital (NBO) analyses, physical and structural properties of Ng_n@C₈₀ and Ng_n@Si₈₀ structures are considered using PBEPBE/6-31G method. It should be noted that the optimized geometries obtained from SIESTA package are used as initial structures for latter calculations. The calculations are carried out by Gaussian03 package [47].

In order to understand the stability of Ng_n@C₈₀ and Ng_n@Si₈₀ complexes, the stabilization energy (E_{stab}) of encapsulated process is defined as:

$$E_{\text{stab}} = E_{\text{Ng}_n \text{@cage}} - (E_{\text{cage}} + nE_{\text{Ng}}) \quad (1)$$

where $E_{\text{Ng}_n \text{@cage}}$ denotes the total energy of Ng_n@C₈₀ and Ng_n@Si₈₀ complexes, and E_{cage} and E_{Ng} are the total energies of the free fullerenes and noble gas molecules respectively. According to the Eq. (1) negative stabilization energy which indicates the formed complex is stable. Also, positive stabilization energy belongs to the local minimum in which the encapsulation of gas molecule into the fullerene cage is prevented by a barrier.

3. Results and discussion

The fully optimized geometries of pure C₈₀ and Si₈₀ are shown in Fig. 1. As it can be seen in Fig. 1, the relax geometry of Si₈₀ distorts cage-like fullerene with inflected C_{2v} symmetry. The Si atom does not form stable fullerene like structures, mainly because of its unfavorable sp² hybridization. Because of its sp³ hybridization in the bulk, Si, when used in fullerenes, it prefers to form dangling bonds rather than single/doublet bonds across the pentagon and hexagon rings. On the other hand, the optimized geometry of C₈₀ was found to be D_{5d} symmetry. The calculated average single C–C bond of C₈₀ is found to be 1.45 Å and for the double bond of C₈₀ molecule, the C–C bond is found to be 1.42 Å, which are in well agreement with the other research work [48]. Besides, the final optimization geometry of Si₈₀ fullerene show that two-disordered boat conformers (~101.2°) in each corner of Si₈₀ cage. It is important to remark that the pure silicon cage clusters are unstable due to the lack of sp² bonding in silicon [49,50]. The calculated average Si–Si bond of Si₈₀ is found to be 2.34 Å. The obtained data are in well agreement with the other research work [51]. We report noble gas atoms encapsulated in C₈₀ and Si₈₀ fullerenes as given by the general formula Ng_n@C₈₀ and Ng_n@Si₈₀, when n is the number of noble gas atoms. For this purpose, we randomly scrambled the number of gas atoms inserted to the fullerene C₈₀ and Si₈₀ cages and then the complex resulted are optimized without any symmetry restriction using PBE/DZP level of theory. The number of internal helium, neon and argon atoms inserted to the C₈₀ cage is ranged from 15 to 55, 20 to 25 and 10 to 15 for helium, neon and argon respectively. In addition, in the case of Si₈₀ fullerene, the number of encapsulation of helium, neon and argon molecules go from 15 to 100, 15 to 58 and 5 to 23 atoms correspondingly. The latter number of n is defining as the maximum number of each Ng atoms can be trapped into the C₈₀ and Si₈₀ fullerenes. The maximum storage capacity is defined as the maximum number of noble gas atoms which can be inserted into the fullerene cage before the bond breaking is occurred in the C₈₀ and Si₈₀ structures.

3.1. Geometry of helium, neon and argon gases encapsulated in the C₈₀ fullerene

To investigate the stability of formed complexes, the stabilization energy of Ng_n@C₈₀ is calculated using Eq. (1). The dependence of the stabilization energy on n is shown in Fig. 2. First, we checked the variation of E_{stab} of Ng_n@C₈₀ structures versus n . According to Fig. 2, we can observe that the stabilization energy of the Ng_n@C₈₀

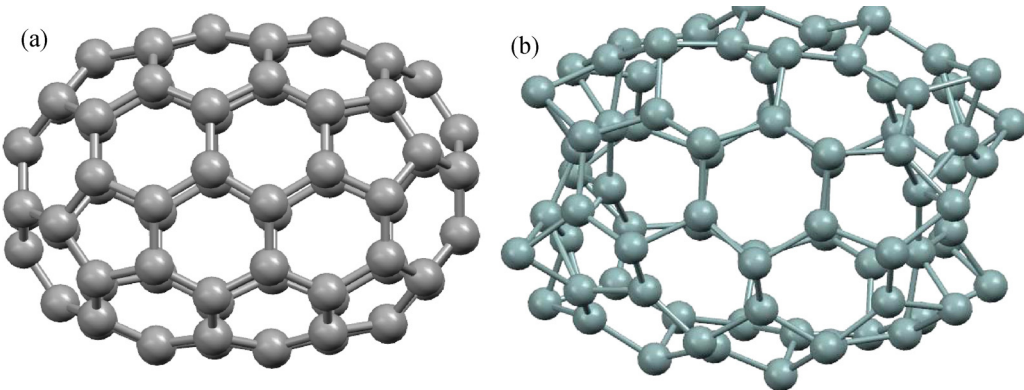


Fig. 1. Optimized geometry of pure (a) C_{80} and (b) Si_{80} fullerenes using PBE/DZP level of theory.

complexes is augmented by increasing the number of gas atoms. Fig. 2 illustrates that the E_{stab} of $Ng_n@C_{80}$ structures has positive value in all cases, which indicates that the formed structures are metastable. It should be stated that, although some of these structures are highly endothermic and unlikely to form, they still correspond to the local minima of potential energy surface. These results are also in accordance with other research works [48,52,53]. As it is shown in Fig. 2, the stabilization energy of $He_n@C_{80}$ is enhanced by increasing the number of helium atoms. Results show that the maximum number of helium atom can be trapped into the

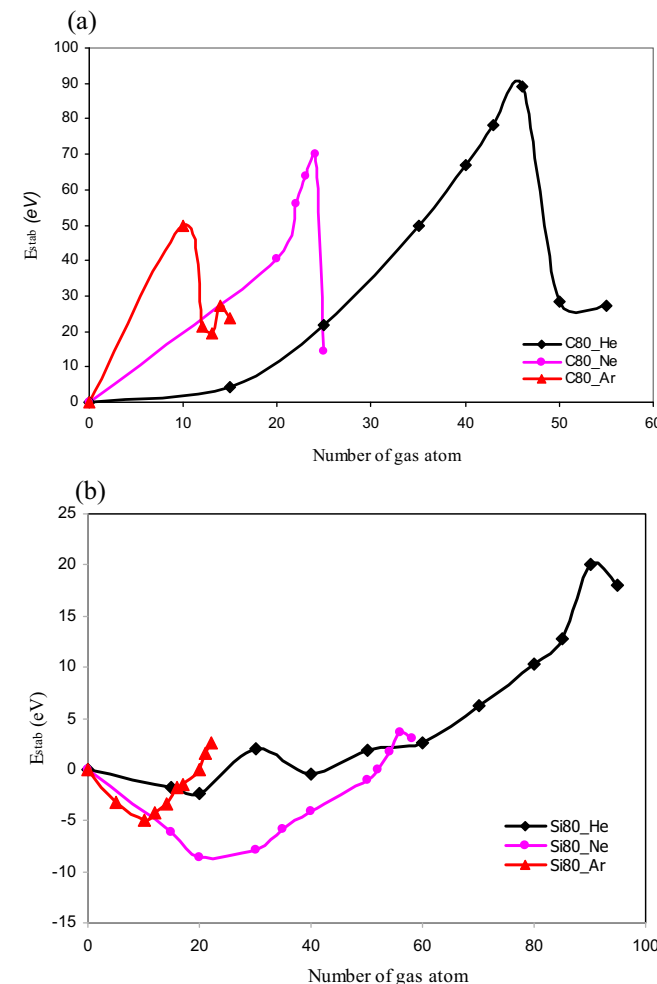


Fig. 2. Formation energy versus number of encapsulated noble gas atoms in (a) $Ng_n@C_{80}$ and (b) $Ng_n@Si_{80}$ structures.

C_{80} fullerene is 46 atoms, whereas no bond breaking is occurred. Tonner et al. [27] showed that the maximum number of helium atoms which can be trapped in C_{60} cage is 40 atoms. The helium atom content of $He_{46}@C_{80}$ metastable structure with huge stabilization energy of 90 eV, is approximately 19.16%. In comparison, Pupysheva et al. [48] reported that the maximum hydrogen content of $H_{56}@C_{60}$ is approximately 7.5%, which formally exceeds the U.S Department of Energy (DOE) target for the year 2010.

In Fig. 3 the representative results of the PBE equilibrium configurations for 15, 25, 46, 50 and 55 helium atoms encapsulated in C_{80} cage are shown. In other words, Fig. 3 shows the mechanism of cage opening of C_{80} . If the number of helium atom inserted to the C_{80} is more than 46 atoms, the stabilization energy is decreased because the C–C bond of fullerene is broken and the gas atom can be escaped from the nanocage (see Fig. 3). For example, if the number of the helium atom is increased to 50, the C–C bonds of C_{80} are broken and the helium atom escaped from the fullerene cage (see Fig. 3). It is worth mentioning that the final optimization of $He_{50}@C_{80}$ structure is especially interesting; this structure is similar to shopping cart; therefore, we named this structure “Molecular Cart” because of its similarity to shopping cart. It is noteworthy that this structure is reported for the first time. As shown in Fig. 3(d) when the number of helium atom increased to 56, the molecular cart is disappeared. It can be concluded that the maximum number of helium atoms can be stored in the C_{80} fullerene cage is 46 atoms.

Alternatively, we can see that the encapsulated helium atoms inside of the fullerene are not adsorbed to the internal surface of the fullerene. By increasing n , the density of helium atom is increased, while the volume of fullerene cage expands slowly. Therefore, the various C–C bonds in the fullerene cage are gradually expanded as function of the number of stored helium atoms inside fullerene. At the high density of the helium atom inside of the fullerene, the average C–C bonds are obtained as 1.617 and 1.445 Å for the single and double bonds of C–C respectively (see Table S1 in Supplementary Data). It can be claimed that our obtained results are consistent with the work done by Barajas-Barraza and Guirado-Lopez [54]. Moreover they considered the effective hydrogen storage in the structural parameters of C_{60} and C_{80} . Our calculations prove that the nearest neighbor of He–He bond is vary from 1.852 to 1.560 Å for low and high density of helium atom inside of fullerene. Also, the closest intermolecular distance between helium atom and internal surface of the fullerene is calculated as approximately 2.127 Å (see Table S1).

In the case of encapsulated neon and argon atoms, we also determined how many neon and argon atoms could be trapped inside of fullerene cage. For the neon atom, like helium, the stabilization energy of $Ne_n@C_{80}$ structures is enhanced by increasing n . Also, the maximum neon atoms which can be stored in the fullerene cage are obtained 24 atoms. The obtained stabilization energy of latter

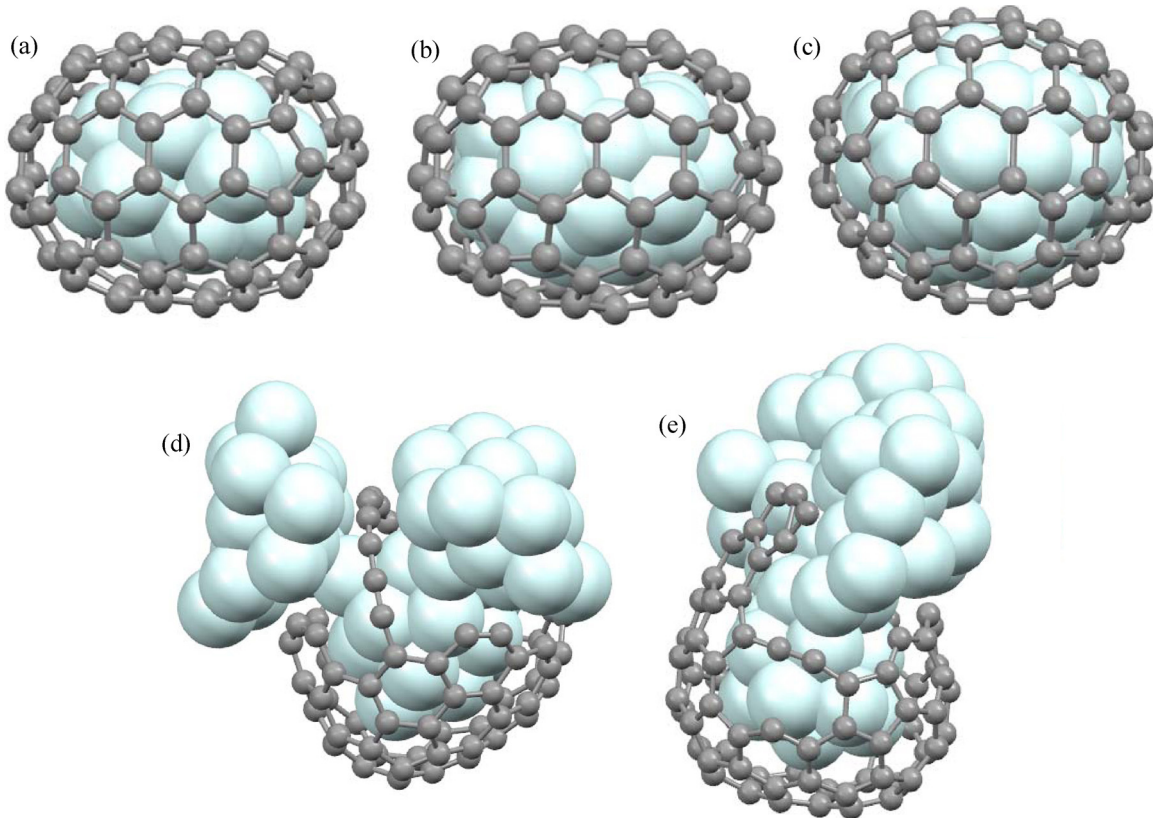


Fig. 3. Typically optimized geometries of encapsulated helium atoms for (a) $\text{He}_{15}@\text{C}_{80}$, (b) $\text{He}_{25}@\text{C}_{80}$, (c) $\text{He}_{46}@\text{C}_{80}$, (d) $\text{He}_{50}@\text{C}_{80}$ and (e) $\text{He}_{55}@\text{C}_{80}$.

structure is ~ 70 eV. We found that the average C–C bond of C_{80} in the $\text{Ne}_n@\text{C}_{80}$ structures is ~ 1.689 and 1.445 Å for the single and double bonds respectively. Furthermore, the nearest intermolecular distances of Ne–Ne and Ne–C are about 2.025 and 2.053 Å correspondingly (see Table S1). By increasing the number of neon atom to 25 , the C–C bond of fullerene is broken and the neon atom could be released from the nanocage. In the final optimization geometry of the $\text{Ne}_{25}@\text{C}_{80}$ structure, we could not see the molecular cart structure similar to the $\text{He}_{50}@\text{C}_{80}$ structure. The final optimization geometries of $\text{Ne}_n@\text{C}_{80}$ and the cage opening mechanism of these structures are represented in Fig. 4(a)–(d).

In continue the encapsulation of argon atom into the C_{80} cage is investigated. The maximum number of argon atom which could be stored into the nanocage is found to be 10 molecules. The average C–C bonds of C_{80} in the $\text{Ar}_n@\text{C}_{80}$ structures are obtained 1.744 and 1.437 Å for the single and double bonds respectively. Moreover, the nearest intermolecular distances of Ar–Ar and Ar–C are calculated about 2.35 and 2.275 Å correspondingly. The structural parameters are collected in Table S1 in Supplementary Materials. If the number of argon atom reached to 12 , the C–C bond breaking is occurred and gas atom can be thrown off the fullerene cage. It should be asserted that the $\text{Ar}_{13}@\text{C}_{80}$ structure formed the molecular cart similar to $\text{He}_{50}@\text{C}_{80}$ structure (see Fig. 4). Considering aforementioned results, it is thus evident that repulsive interactions during the encapsulation of Ng atom and the fullerene wall, as well as between various Ng atoms play an important role in determining the Ng storage capacity in the C_{80} nanocage.

It is well known that the most compact forms maximizing the number of bonds between the cluster atoms of Ng are represented by Lennard-Jones (LJ) structure, for which a wide range of global minima has been compiled [27,54]. The cluster structures of Ng_n obtained from the optimized $\text{Ng}_n@\text{C}_{80}$ complexes are depicted in Fig. 5 for various n . The Ng atoms inside of the

C_{80} fullerene arrange themselves in well-defined configurations, namely, bicapped square antiprismatic and icosahedral clusters. For higher number of noble gas atoms that defines a relatively large density of encapsulated Ng in fullerene, a considerable distorted icosahedral-like structure is found (see Fig. 5).

3.2. Geometry of helium, neon and argon gases encapsulated in the Si_{80} fullerene

Fig. 2(b) represents the variation of stabilization energy versus n for encapsulation of He, Ne and Ar atoms into the Si_{80} fullerene. As illustrated in Fig. 2(b), firstly the stabilization energy of $\text{Ng}_n@\text{Si}_{80}$ structures is gradually decreased as the n increases, which indicates that the formed structures become increasingly stable rather than pure Si_{80} fullerene. In other words, these configurations are truly energetically favorable. As we know the pure hollow silicon cage is known to be unstable. In other words, encapsulation of low density of noble gases can stabilize the Si_{80} fullerene. It was found that when $n \leq 30, 52$ and 12 for helium, neon and argon respectively, the whole $\text{Ng}_n@\text{Si}_{80}$ system are truly energetically favorable and the stabilization energies are negative. By increasing n ($n \geq 30, 52$ and 12 for helium, neon and argon respectively), the stabilization energy goes to the positive values which means that the $\text{Ng}_n@\text{Si}_{80}$ structures, with the latter n , are metastable with high value in stabilization energy. Meanwhile, the highest stability of $\text{Ng}_n@\text{Si}_{80}$ structures are related to the $n = 20, 20$ and 10 for helium, neon and argon correspondingly. For helium encapsulation, the stabilization energy of $\text{He}_{20}@\text{Si}_{80}$ system has ~ -2.364 eV. The fully optimized geometries for various n ($15, 20, 30, 40, 60, 70, 90$ and 95) helium atoms encapsulated in Si_{80} cage are represented in Fig. 6. By inserting helium into Si_{80} cage, results indicate that the maximum number of helium atoms can be inserted into the Si_{80} without any bond breaking is 95 atoms. The $\text{He}_{95}@\text{Si}_{80}$ metastable structure has

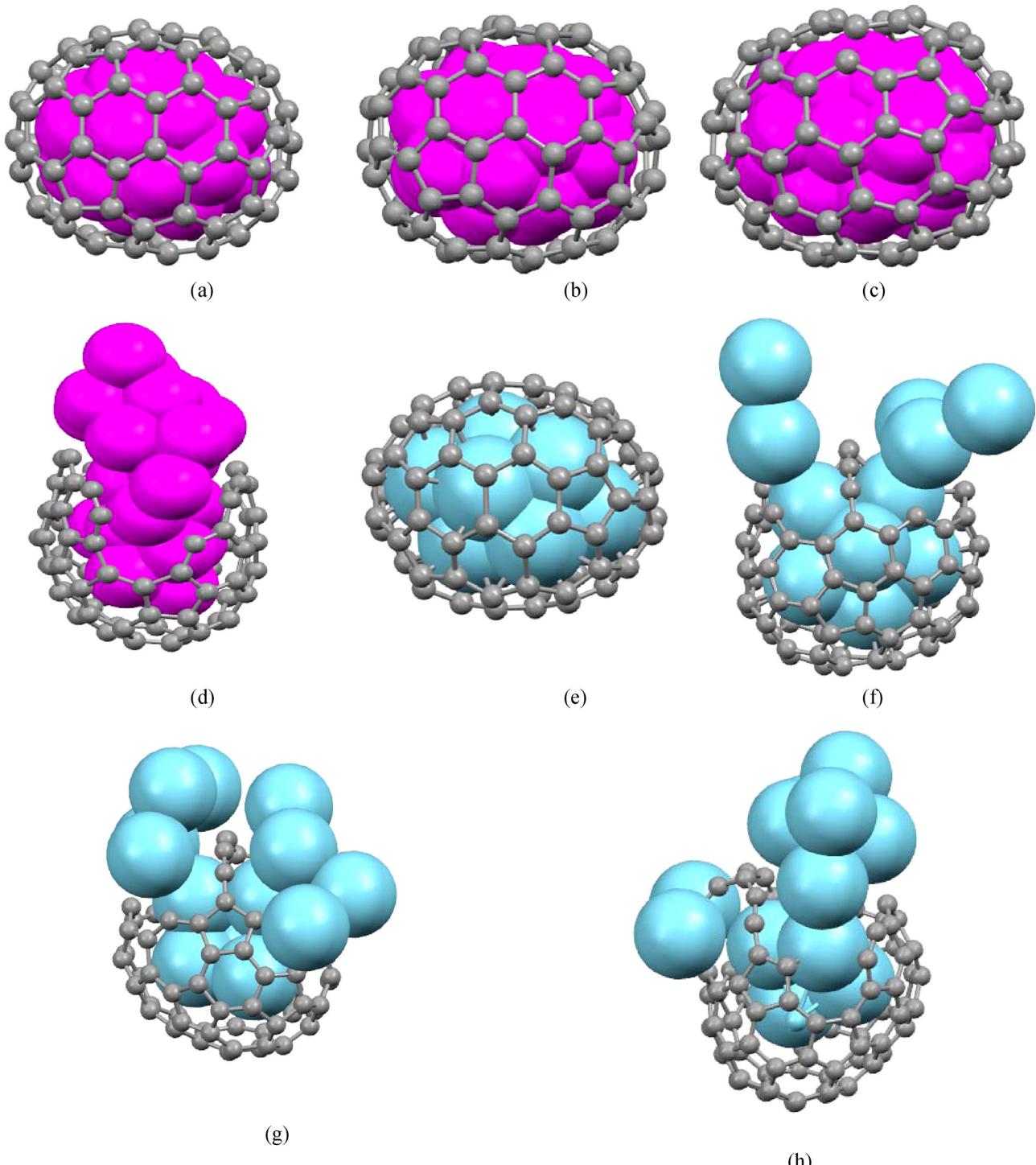


Fig. 4. Typically optimized geometries of encapsulated neon atoms for (a) $\text{Ne}_{20}@\text{C}_{80}$, (b) $\text{Ne}_{22}@\text{C}_{80}$, (c) $\text{Ne}_{24}@\text{C}_{80}$, (d) $\text{Ne}_{25}@\text{C}_{80}$, (e) $\text{Ar}_{10}@\text{C}_{80}$, (f) $\text{Ar}_{12}@\text{C}_{80}$, (g) $\text{Ar}_{13}@\text{C}_{80}$ and (h) $\text{Ar}_{14}@\text{C}_{80}$.

large stabilization energy of about 18 eV. The helium atom content of this structure is approximately 16.92%. If the number of helium atom trapped to the Si_{80} is increased (reach to 100 atoms), the Si–Si bond of fullerene is broken and the gas atom can be escaped from the nanocage. Therefore, the stabilization energy of this structure goes to the positive value, which means the stability is decreased (Fig. 2(b)).

According to Fig. 6, it can be seen that, the encapsulated helium atoms inside of the Si_{80} in more cases are not adsorbed into the internal surface of Si_{80} . By increasing n , the density of helium atom

is increased, while the fullerene cage expands slowly. Alternatively, the Si–Si bonds in Si_{80} fullerene are gradually expanded as a function of number of encapsulated helium atoms. In high density of helium atom, the average Si–Si bond is obtained 2.40 Å as well as the nearest intermolecular distance between He–Si is obtained about 2.436 Å. Furthermore, the nearest intermolecular distance of He–He is vary from 2.120 to 1.85 Å for low and high density of helium atom respectively (see Table S1). It should be reminded that the encapsulated of helium atoms into the Si_{80} are in the cluster form which is depicted in Fig. S1 in Supplementary Materials.

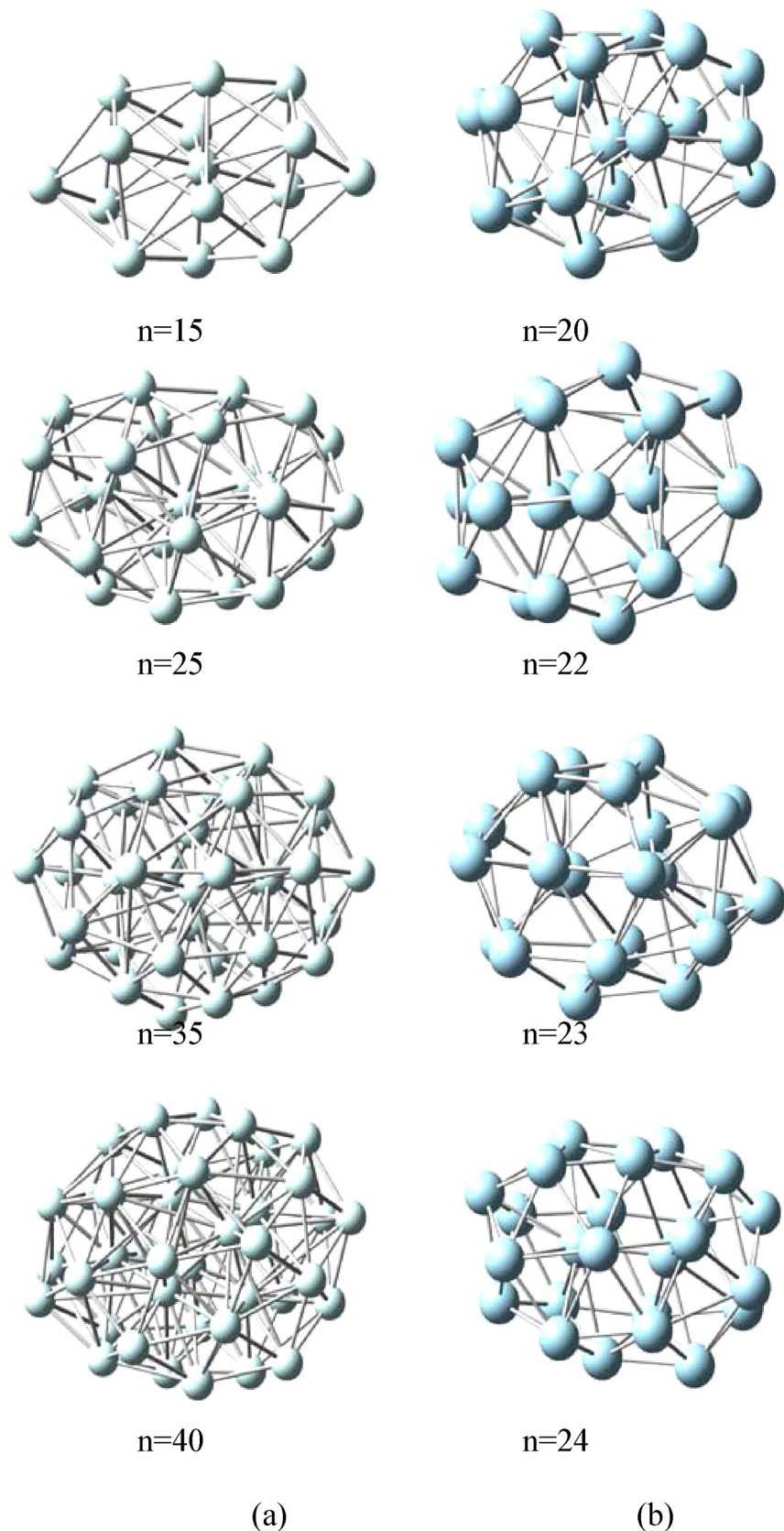


Fig. 5. Ng_n clusters obtained from optimized geometries of $Ng_n@C_{80}$ structures for various n ; in first columns (a) $Ng=He$ and in second columns (b) $Ng=Ne$. Clusters for the argon atom are similar.

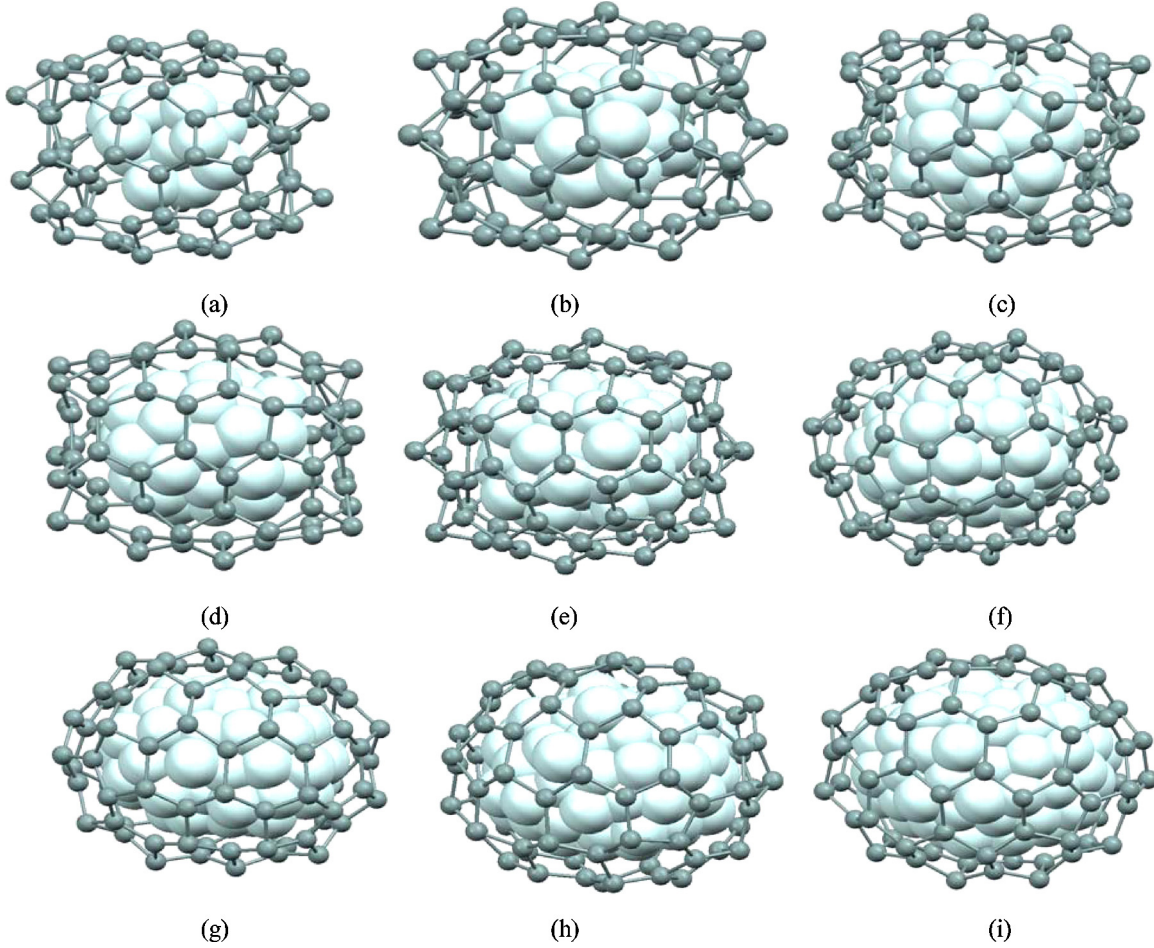


Fig. 6. Typically optimized geometries of encapsulated helium atoms for (a) $\text{He}_{15}@\text{Si}_{80}$, (b) $\text{He}_{20}@\text{Si}_{80}$, (c) $\text{He}_{30}@\text{Si}_{80}$ and (d) $\text{He}_{40}@\text{Si}_{80}$, (e) $\text{He}_{50}@\text{Si}_{80}$, (f) $\text{He}_{60}@\text{Si}_{80}$ and (g) $\text{He}_{70}@\text{Si}_{80}$, (h) $\text{He}_{90}@\text{Si}_{80}$, (i) $\text{He}_{95}@\text{Si}_{80}$.

Because our aim was to explore how many noble gas atoms can be inserted into the Si_{80} nanocage, it was crucial to know the maximum number of neon and argon gas atoms into the Si_{80} fullerene cage. Fig. 2(b) shows the variation of stabilization energy of $\text{Ne}_n@\text{Si}_{80}$ and $\text{Ar}_n@\text{Si}_{80}$ structures as a number of gas atoms trapped into the fullerene cage. As seen there, the stabilization energy is firstly decreased (goes to the negative values) by increasing n . In other words, for small number of n , encapsulation of noble gases into the fullerene cage is favorable. It has to be highlighted that this general trend is also observed for the encapsulation of helium atoms into the Si_{80} fullerene. As already mentioned in previous section, when the number of inserted gas atoms is increased the stabilization energy is increased as well (goes to the positive values), which is shown that the stability of formed structures is decreased. In addition, results indicate that the $\text{Ne}_{20}@\text{Si}_{80}$ and $\text{Ar}_{10}@\text{Si}_{80}$ structures are the most stable than those others. By increasing the number of n , the cavity of the fullerene is also gradually increased. Hence, the curvature of the inner surface of fullerene creates a repulsive interaction between the surface of the fullerene and noble gas atoms, therefore, the stabilization energy is increased.

The gas atoms encapsulated into the Si_{80} can affect the structural parameters of fullerene. We found that the average Si–Si bonds of Si_{80} in the $\text{Ne}_n@\text{Si}_{80}$ structures are 2.373 \AA . In this case, the nearest intermolecular of Ne–Ne and Ne–Si bonds are about 2.385 and 2.853 \AA respectively. The maximum number of neon atom which could be trapped into C_{80} nanocage is found to be 56 neon atoms and the structure still remained a metastable structure. When the

number of neon atoms reached to 58 , the Si–Si bond is broken and then a neon atom could be escaped from the nanocage. The final optimization geometry of $\text{Ne}_n@\text{Si}_{80}$ (or mechanism of cage opening) is depicted in Fig. 7.

In the case of argon, the maximum number of gas atom could be stored into the nanocage which is found to be 22 atoms. The relaxed geometry of $\text{Ar}_n@\text{Si}_{80}$ is presented in Fig. 8. It is appealing to note that when the number of argon atoms reached to 23 , the bond breaking is occurred and three argon atoms throw off the cage. After this, the distorted Si_{80} fullerene tried to mend the broken bonds, and could fix some of them. This led us to investigate the new structure of $\text{Ar}_n@\text{Si}_{80}$. For this purpose, we inserted 20 foreign atoms into the Si_{80} fullerene. These foreign atoms contain 19 argon and one Si atoms. In other words, we investigate the $\text{Ar}_{19}@\text{Si}_{81}$ structure. It should be mentioned that the additional Si atom, randomly inserted into the $\text{Ar}_{19}@\text{Si}_{80}$ structure. After full optimization, relaxed geometry of $\text{Ar}_{19}@\text{Si}_{81}$ showed that the additional Si atom migrate from the cavity to the inner surface of the Si_{80} and attached to the three Si atoms of cage. During the optimization processes, the Si–Si bond is broken and two argon atom escape from the cage. After that the fullerene cage completely rebuilds its structure like the initial one. This phenomenon is similar to cesarean section; therefore, we named this observation *Molecular Cesarean Section*. It is remarkable that this phenomenon is also reported for the first time. The mechanism of molecular delivery of argon atom from $\text{Ar}_{19}@\text{Si}_{81}$ structure is depicted in Fig. 9.

Results indicate that the presence of encapsulated gas atoms into the fullerene cage impacts the Si–Si bond lengths. In other

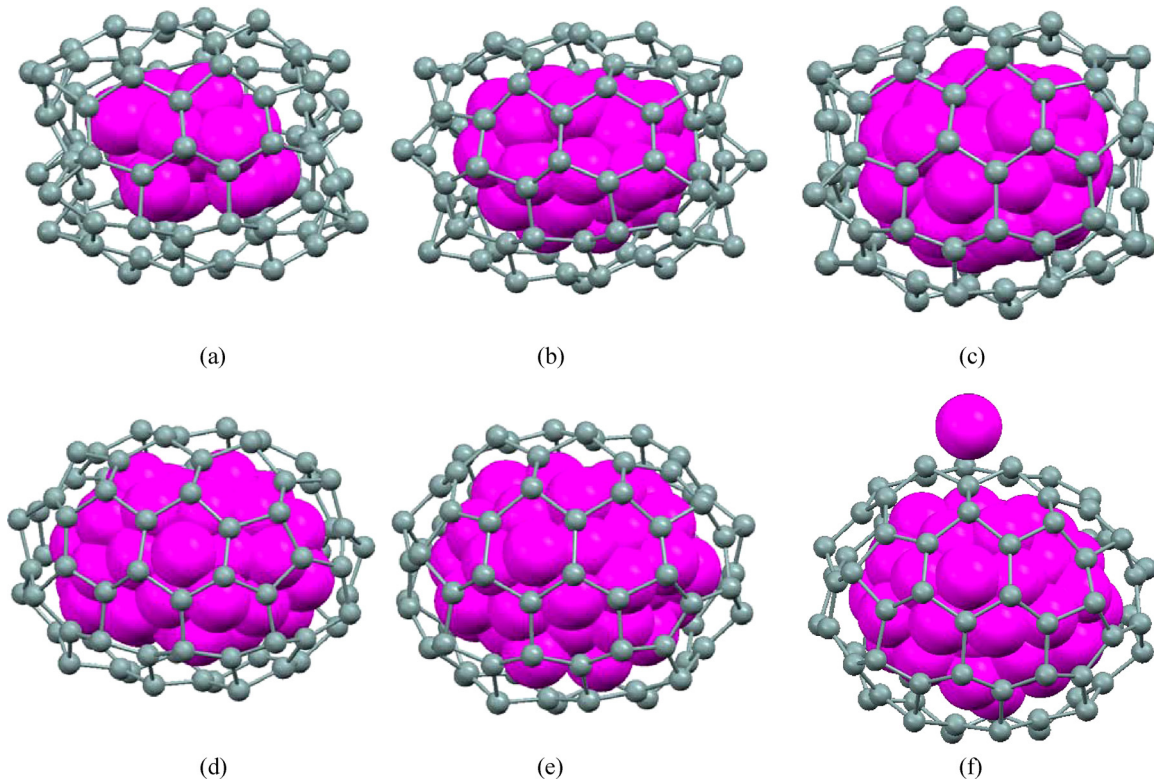


Fig. 7. Typically optimized geometries of encapsulated neon atoms for (a) $\text{Ne}_{15}@\text{Si}_{80}$, (b) $\text{Ne}_{30}@\text{Si}_{80}$, (c) $\text{Ne}_{40}@\text{Si}_{80}$, (d) $\text{Ne}_{50}@\text{Si}_{80}$, (e) $\text{Ne}_{56}@\text{Si}_{80}$ and (f) $\text{Ne}_{58}@\text{Si}_{80}$.

words, the cavity of Si_{80} fullerene is slowly increased by increasing the number of encapsulated gas atoms. The average Si–Si bonds in the $\text{Ar}_n@\text{Si}_{80}$ structures are obtained 2.395 Å. Also, the average of nearest intermolecular of Ar–Ar and Ar–Si bonds are about 2.985 and 2.975 Å respectively. The structural parameters are collected in Table S1. Based on the results one can clearly conclude that repulsive interactions during the encapsulation of Ng molecule and the fullerene wall, as well as among various Ng atoms play an important role in determining the Ng storage capacity in the Si_{80} cage.

3.3. Calculated cavity volume and internal pressure of $\text{Ng}_n@\text{C}_{80}$ and $\text{Ng}_n@\text{Si}_{80}$ structures

Monte-Carlo method of calculating is used to calculate the cage volume of $\text{Ng}_n@\text{C}_{80}$ and $\text{Ng}_n@\text{Si}_{80}$ structures. All calculation is performed with Gaussian 03 package. Calculating the cage volume returns value of 842.58 and 2198.68 Å³ for the relaxed C_{80} and Si_{80} structures. The dependence cage volume of $\text{Ng}_n@\text{C}_{80}$ and $\text{Ng}_n@\text{Si}_{80}$ structures on n is shown in Fig. 10. Based on this figure, it can be seen that, the C_{80} cage volume is monotonically increased by increasing the number of encapsulated gas atoms. At maximum load of Ng atom, results show a large increase in volume, up to 8.06% relative to the pristine C_{80} before bond breaking. In the case of Si_{80} , we do not observe general trend between $\text{Ng}_n@\text{Si}_{80}$ cage volume and n (number of gas atom). Results indicate that the maximum change in the cage volume is calculated about 36.94% relative to the pure Si_{80} cage. The increasing cage volumes is in fact the outcome of two opposing driving forces long range dispersion and short range Pauli repulsion [55]. The short range repulsion between noble gas atom and silicon or carbon atoms should lead to cage expansion.

The large computed volumes of the cages together with the elongated C–C and Si–Si bond distances and the extremely unfavorable stability energies indicate that the encapsulation of such a large number of Ng atoms distorts the fullerene cage quite substantially. The distortion energy [56], also called deformation energy [56,57]

of fullerene is also calculated. Fullerene deformation energy due to the presence of the gas cluster, calculated as the energy difference between the distorted geometry of fullerenes in the $\text{Ng}_n@\text{Si}_{80}$ or $\text{Ng}_n@\text{C}_{80}$ structures and the optimized geometry of free fullerene at the PBEPBE/6-31G level of theory. The deformation energies of investigated structures are summarized in Tables 1 and 2 and also plotted in Fig. 11. According to these results, it is clear that the curvature in the geometry of C_{80} and Si_{80} cages are occurred when gas atoms inserted into the fullerene cages. In the case of C_{80} , our results indicated that the deformation energy of $\text{Ng}_n@\text{C}_{80}$ structures has positive value in all cases which indicate that the formed structures are metastable (see Table 1). As can be seen in Fig. 11(a), when the number of gas atom is increased the value of deformation energy is also increased, which leads to increase the cage volume of C_{80} . Fig. 11(b) illustrates that the deformation energy of $\text{Ng}_n@\text{Si}_{80}$

Table 1

Calculated deformation energy (ΔE_{deform}) and charge transferred to the fullerene cage in the $\text{Ng}_n@\text{C}_{80}$ structures using PBEPBE/6-31G level of theory.

Type	E (hartree)	^b Charge transfer (a.u.)	^a ΔE_{deform} (kJ/mol)
C_{80} free	-3044.2458	0.0	-
C_{80} in $\text{He}_{15}@\text{C}_{80}$	-3044.2352	-0.2588	27.9844
C_{80} in $\text{He}_{25}@\text{C}_{80}$	-3044.1881	-0.5047	151.5783
C_{80} in $\text{He}_{35}@\text{C}_{80}$	-3043.9924	-0.7752	665.4227
C_{80} in $\text{He}_{40}@\text{C}_{80}$	-3043.8259	-0.9130	1102.4422
C_{80} in $\text{He}_{43}@\text{C}_{80}$	-3043.6979	-1.0108	1438.6230
C_{80} in $\text{He}_{46}@\text{C}_{80}$	-3043.5457	-1.0934	1838.1829
C_{80} in $\text{Ne}_{20}@\text{C}_{80}$	-3043.8466	-1.1662	1048.2474
C_{80} in $\text{Ne}_{22}@\text{C}_{80}$	-3043.6871	-1.2759	1466.8981
C_{80} in $\text{Ne}_{23}@\text{C}_{80}$	-3043.5827	-1.3278	1741.1276
C_{80} in $\text{Ne}_{24}@\text{C}_{80}$	-3043.4986	-1.3981	1961.8613
C_{80} in $\text{Ar}_{10}@\text{C}_{80}$	-3043.8441	-0.7025	252.1058

^a $\Delta E_{\text{deform}} = (E_{\text{fullerene in complex}}) - (E_{\text{fullerene free}})$.

^b Charge transferred from the gas cluster to the C_{80} cage measured as the sum of Mulliken charges of all the fullerene carbon atoms obtained at the PBEPBE/6-31G level of theory.

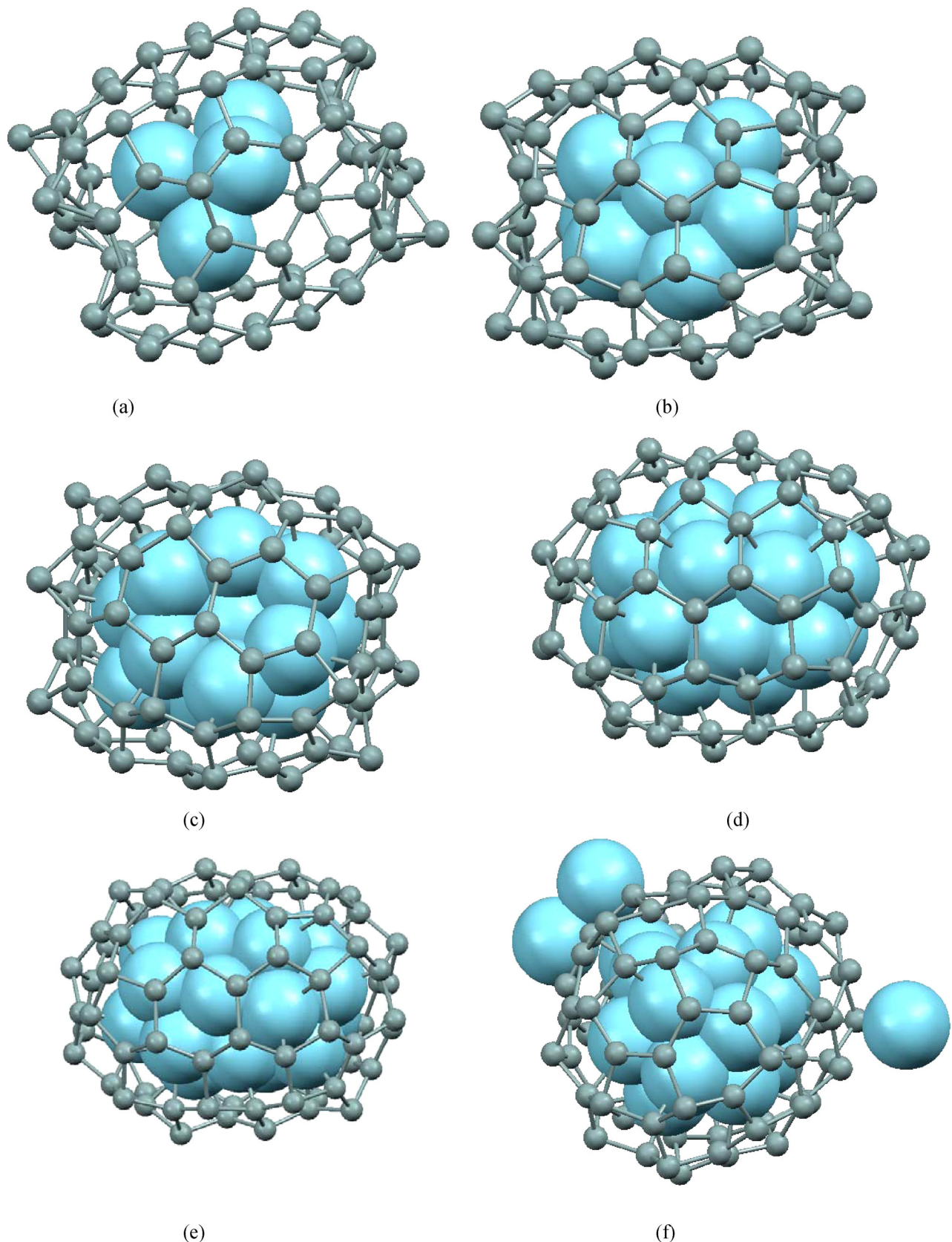


Fig. 8. Typically optimized geometries of encapsulated argon atoms for (a) $\text{Ar}_5@\text{Si}_{80}$, (b) $\text{Ar}_{10}@\text{Si}_{80}$, (c) $\text{Ar}_{16}@\text{Si}_{80}$, (d) $\text{Ar}_{20}@\text{Si}_{80}$, (e) $\text{Ar}_{22}@\text{Si}_{80}$ and (f) $\text{Ar}_{23}@\text{Si}_{80}$.

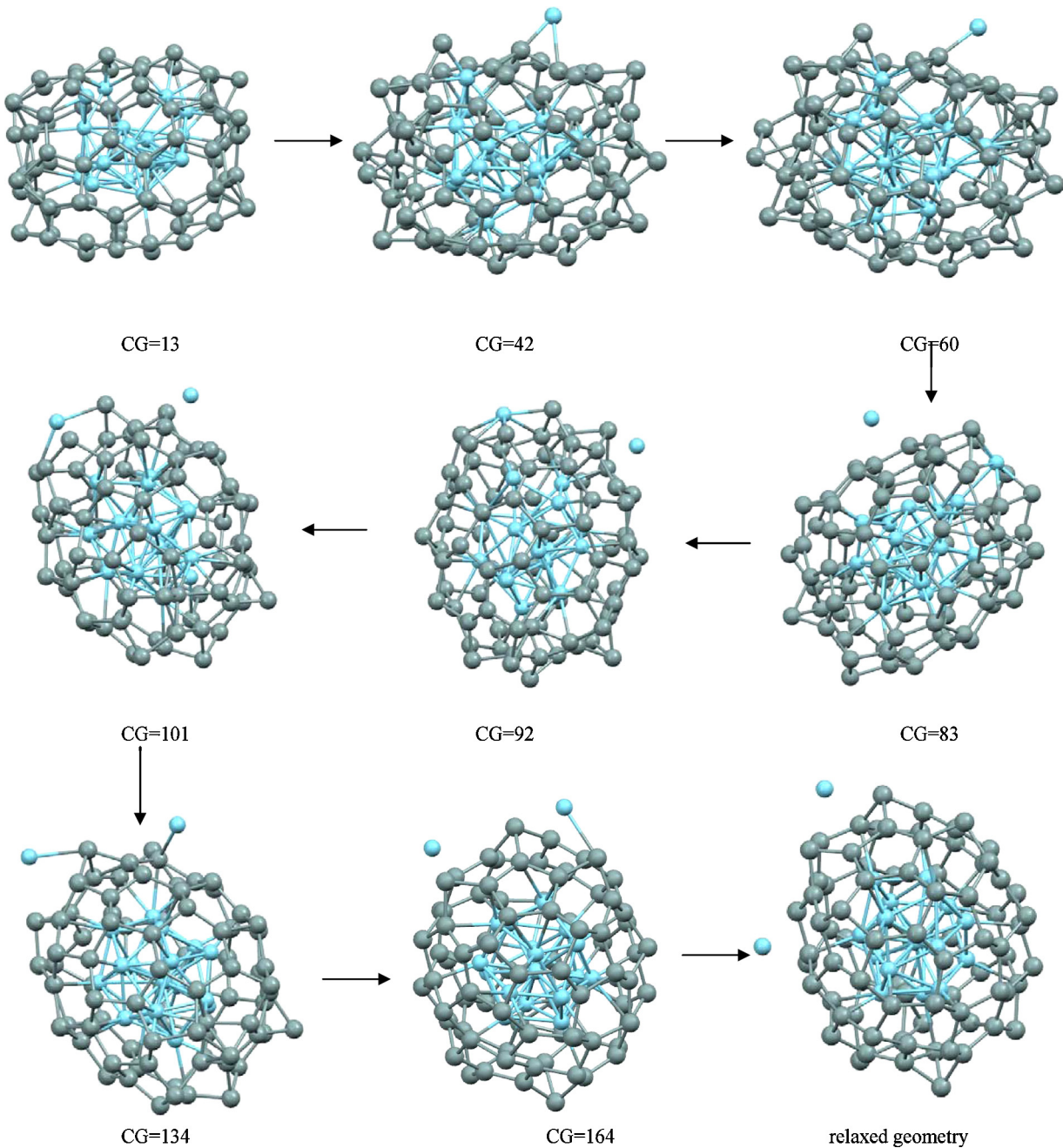


Fig. 9. The mechanism of molecular delivery of argon from $\text{Ar}_{19}@\text{Si}_{81}$ structure using conjugated gradient (CG) algorithm.

structures versus number of gas atoms encapsulation into the Si_{80} fullerene. Unlike C_{80} , the value of deformation energy of Si_{80} cage is decreased with increasing the number of gas atom (see Fig. 11b), which indicates that the formed structures become increasingly stable rather than pure Si_{80} fullerene. As we know the pure hollow silicon cage is known to be unstable. Furthermore, as curvature in the fullerene cages increases, the C–C and Si–Si bonds of C_{80} and Si_{80} become longer and the cage volume goes to larger value in the $\text{Ng}_n@\text{C}_{80}$ and $\text{Ng}_n@\text{Si}_{80}$ structures. In the case of C_{80} , the encapsulation of gas atoms leads to a transformation of the p orbitals to hybrid orbitals, and π bonding is weakened leading to larger C–C bond lengths.

In the following, the internal pressure of Ng atoms in the nanocage is estimated using ideal gas equation of state. The calculated internal pressure of Ng atoms inside of fullerene is plotted against n (see Fig. 12). The pressure calculations are also performed

using virial equation of state. Although usually not the most convenient equation of state, the virial equation is important because it can be derived directly from statistical mechanics. Based on our calculations, there is no significant change observed if the virial equation of state is used to calculate the internal pressure of $\text{Ng}_n@\text{Si}_{80}$ and $\text{Ng}_n@\text{C}_{80}$ structures instead of ideal equation of state (see Fig. S4 in the Supplementary data). The internal pressure of Ng atoms inside of C_{80} and Si_{80} are smoothly increased by increasing the number of gas atoms trapped into the nanocage. For example, the helium pressure in $\text{He}_{46}@\text{C}_{80}$ structure reaches approximately to 212.27 GPa. Also, results reveal that the maximum internal pressure that Si_{80} fullerene can be endured is obtained about 144.10 GPa for $\text{He}_{95}@\text{Si}_{80}$ structure. It should be reminded that no bond breaking is observed for those structures. For the heavier noble gas atoms, the internal pressure is also calculated and the same trends are obtained. It seems useful to shed light on the obtained data by

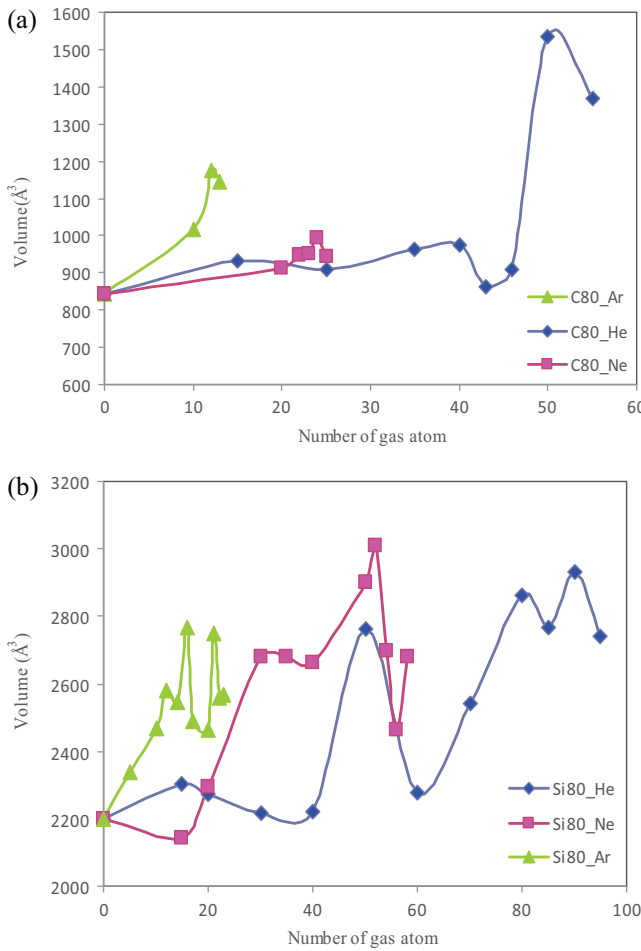


Fig. 10. Calculated cavity volume of (a) $\text{Ng}_n@\text{C}_{80}$ and (b) $\text{Ng}_n@\text{Si}_{80}$ structures versus number of noble gas atom.

comparing our results with the work done by Pupysheva et al. [48]. These authors calculated the internal pressure of hydrogen encapsulated into the C_{60} fullerene and they obtained the 130 GPa for $\text{H}_{56}@\text{C}_{60}$ structure. There is no reference data published so far in the case of noble gas encapsulated into the Si_{80} fullerene for comparing our results with it.

3.4. NBO analysis of $\text{Ng}_n@\text{C}_{80}$ and $\text{Ng}_n@\text{Si}_{80}$ structures

In the last section, the NBO analysis to gain electronic properties of studied structures is also studied. Fig. 13 shows the variation of energy gaps between the highest occupied molecular orbital (HOMO) and lowest unoccupied molecular orbital (LUMO) of the $\text{Ng}_n@\text{C}_{80}$ and $\text{Ng}_n@\text{Si}_{80}$ structures. These results indicate that the HOMO and LUMO orbitals of C_{80} , Si_{80} changed when the Ng atoms encapsulated inside the fullerenes. As it can be seen in this figure, the gap energy of $\text{Ng}_n@\text{C}_{80}$ is increased by increasing the number of stored Ng atoms. The maximum value of gap energy is related to the maximum number of Ng atoms stored in nanocage. For example in the case of helium, the maximum gap energy belongs to $\text{He}_{46}@\text{C}_{80}$ structure. If the number of Ng atoms is increased, the gap energy will be decreased which means that the reactivity of the structures is increased. In other words, the stability of formed structures is decreased. These results are in accordance with the results of the stabilization energy. For $\text{Ng}_n@\text{Si}_{80}$ structures, the energy gap for low density of noble gas atoms is decreased by increasing the number of stored Ng atoms. Meanwhile, for higher number of n , the energy gap is increased. The comparison of the energy

Table 2

Calculated deformation energy (ΔE_{deform}) and charge transferred to the fullerene cage in the $\text{Ng}_n@\text{Si}_{80}$ structures using PBEPBE/6-31G level of theory.

Type	E (hartree)	^b Charge transfer (a.u.)	^a ΔE_{deform} (kJ/mol)
Si_{80} free	-23,145.8878	0.0	—
Si_{80} in $\text{He}_{15}@\text{Si}_{80}$	-23,145.8791	-0.3022	22.8156
Si_{80} in $\text{He}_{20}@\text{Si}_{80}$	-23,145.8879	-0.4205	-0.2339
Si_{80} in $\text{He}_{30}@\text{Si}_{80}$	-23,145.9211	-0.7134	-87.3856
Si_{80} in $\text{He}_{40}@\text{Si}_{80}$	-23,145.9492	-0.9766	-161.1865
Si_{80} in $\text{He}_{50}@\text{Si}_{80}$	-23,145.9692	-1.2247	-213.7803
Si_{80} in $\text{He}_{60}@\text{Si}_{80}$	-23,146.0535	-1.4456	-435.0149
Si_{80} in $\text{He}_{70}@\text{Si}_{80}$	-23,146.0434	-1.7042	-408.4028
Si_{80} in $\text{He}_{85}@\text{Si}_{80}$	-23,145.9729	-1.9756	-223.2746
Si_{80} in $\text{He}_{90}@\text{Si}_{80}$	-23,145.9357	-2.0899	-125.8326
Si_{80} in $\text{He}_{95}@\text{Si}_{80}$	-23,145.8995	-2.1724	-30.5768
Si_{80} in $\text{Ne}_{15}@\text{Si}_{80}$	-23,145.8474	-0.9844	106.0258
Si_{80} in $\text{Ne}_{20}@\text{Si}_{80}$	-23,145.8774	-1.3245	27.2548
Si_{80} in $\text{Ne}_{30}@\text{Si}_{80}$	-23,145.9419	-1.9119	-141.9847
Si_{80} in $\text{Ne}_{35}@\text{Si}_{80}$	-23,145.9597	-2.1958	-188.8052
Si_{80} in $\text{Ne}_{40}@\text{Si}_{80}$	-23,145.9535	-2.3708	-172.5279
Si_{80} in $\text{Ne}_{50}@\text{Si}_{80}$	-23,146.0247	-2.7350	-359.3703
Si_{80} in $\text{Ne}_{52}@\text{Si}_{80}$	-23,145.9862	-2.8198	-258.2476
Si_{80} in $\text{Ne}_{54}@\text{Si}_{80}$	-23,145.9805	-2.9199	-243.3686
Si_{80} in $\text{Ne}_{56}@\text{Si}_{80}$	-23,145.9520	-2.9781	-168.6225
Si_{80} in $\text{Ar}_{10}@\text{Si}_{80}$	-23,145.9058	-0.8283	-47.1695
Si_{80} in $\text{Ar}_{12}@\text{Si}_{80}$	-23,145.9251	-0.9953	-97.9973
Si_{80} in $\text{Ar}_{14}@\text{Si}_{80}$	-23,145.9407	-1.2004	-138.8823
Si_{80} in $\text{Ar}_{16}@\text{Si}_{80}$	-23,145.9459	-1.3889	-152.5347
Si_{80} in $\text{Ar}_{17}@\text{Si}_{80}$	-23,145.9438	-1.4148	-146.8946
Si_{80} in $\text{Ar}_{20}@\text{Si}_{80}$	-23,145.9085	-1.8397	-54.4264

^a $\Delta E_{\text{deform}} = (E_{\text{fullerene in complex}}) - (E_{\text{fullerene free}})$.

^b Charge transferred from the gas cluster to the Si_{80} cage measured as the sum of Mulliken charges of all the fullerene carbon atoms obtained at the PBEPBE/6-31G level of theory.

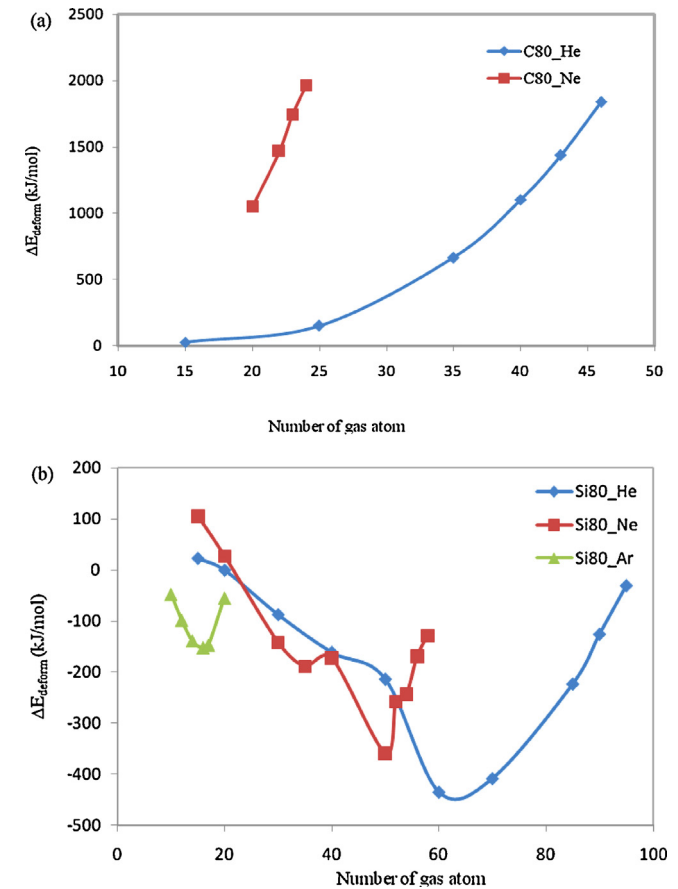


Fig. 11. Calculated deformation energy of $\text{Ng}_n@\text{C}_{80}$ and (b) $\text{Ng}_n@\text{Si}_{80}$ structures versus number of encapsulated noble gas atoms at the PBEPBE/6-31G level of theory.

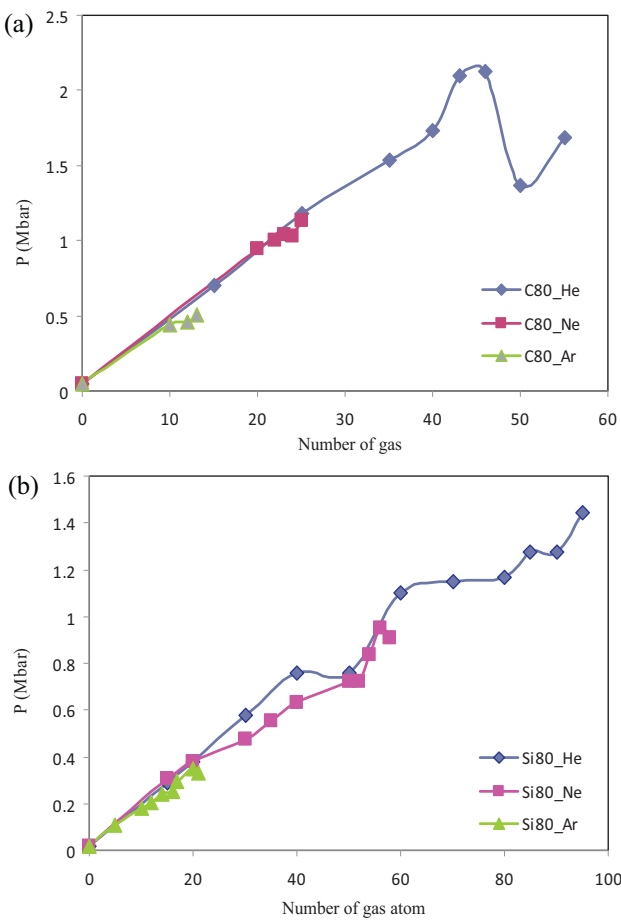


Fig. 12. Calculated internal noble gas pressure on C_{80} and Si_{80} cages versus number of encapsulated noble gas atoms in (a) $\text{Ng}_n\text{@C}_{80}$ and (b) $\text{Ng}_n\text{@Si}_{80}$ structures.

gaps of $\text{Ng}_n\text{@Si}_{80}$ with $\text{Ng}_n\text{@C}_{80}$ structures indicates that they have different behavior since the $\text{Ng}_n\text{@Si}_{80}$ configurations for low density of noble gas atoms are truly energetically more favorable than $\text{Ng}_n\text{@C}_{80}$.

In continue, the analysis of the charge transfer from the Ng clusters to the fullerene cage is also considered. The charge transferred from the gas cluster to the C_{80} and Si_{80} cage measured as the sum of Mulliken charges of all the fullerene carbon and fullerene silicon atoms obtained at the PBE/PBE/6-31G level of theory. These results are summarized in Tables 1 and 2 and Figs. S5 and S6. As seen from these results, significant charge transfer from Ng clusters to fullerene cage is occurred. In the case of $\text{He}_n\text{@C}_{80}$ structures, at high density of helium atom the charge transferred from gas clusters to the C_{80} cage is large whereas for low density of helium atom, the charge transfer is close to zero. Furthermore, the value of charge transferred from gas clusters to the C_{80} cage is obtained in the range of the 0.259–1.0934(a.u.), which means that the total charge of the He_n clusters at the PBE/PBE/6-31G level is +0.259–+1.0934. It should be noted that these values of charge transferred is corresponding to the $\text{He}_{15}\text{@C}_{80}$ – $\text{He}_{46}\text{@C}_{80}$ structures. By changing the Ng from helium to neon, charge transfer becomes more significant. For example, if the number of neon atom is reach to 24, the maximum charge transferred from gas cluster to the C_{80} cage is take place (~ 1.398 a.u.). This trend is also observed for the argon encapsulation (see Table 1). Fig. S5 in supplementary data shows the partial charge distribution on C_{80} and $\text{Ng}_n\text{@C}_{80}$ structures. It is noteworthy that these results are in accordance with results of the other researches [26,58]. Krapp and Frenking [26] observed that the sum of atomic charges of the Xe_2 moiety is +1.06 at the BP86/TZVPP

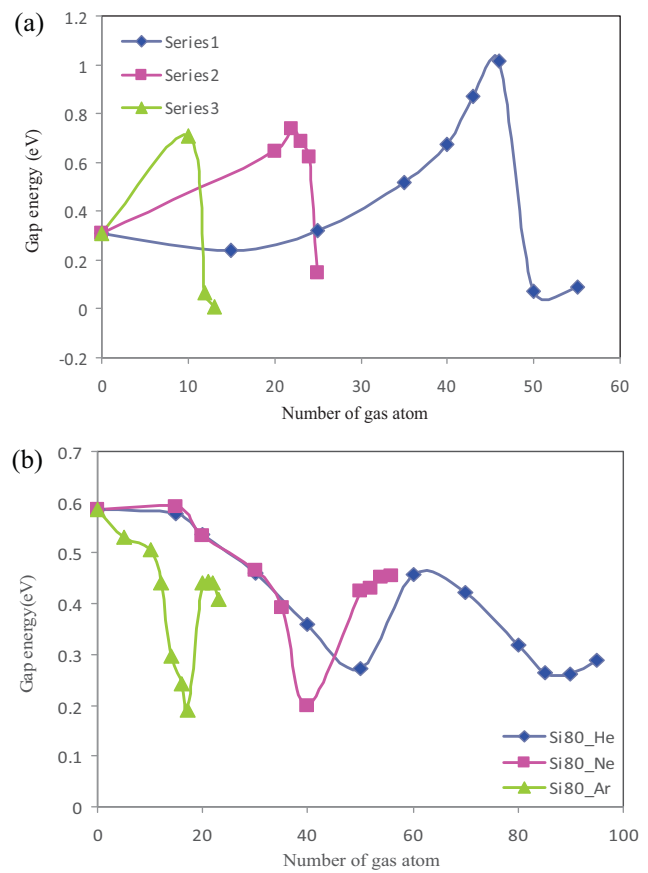


Fig. 13. Calculated energy gap of (a) $\text{Ng}_n\text{@C}_{80}$ and (b) $\text{Ng}_n\text{@Si}_{80}$ structures versus number of encapsulated noble gas atoms.

level in the lowest lying singlet state, that is, about one electron is transferred from the noble gas dimer to the fullerene cage.

In the case of Si_{80} fullerene, the charge transfer to Si_{80} is significantly more than that of C_{80} due to the lack of sp^2 bonding in silicon cage. The calculated charge distribution of $\text{He}_n\text{@Si}_{80}$ structures indicate that the large value of charge (0.3022–2.172) transferred to the Si_{80} cage during the helium encapsulation (see Table 2). As can be seen in Table 2, with increasing the number of encapsulated helium atom into the Si_{80} cage, the value of charge transferred is increased. On the other hand, for neon clusters, transfer of 1–3 electrons from gas clusters to the Si_{80} fullerene takes place. Furthermore, for argon clusters, 1–2 electrons are transferred to the fullerene cage. It should be reminded that the maximum number of helium, neon and argon atoms can encapsulate into the Si_{80} is 95, 56 and 22 respectively. Fig. S6 shows the partial charge distribution on Si_{80} and $\text{Ng}_n\text{@Si}_{80}$ structures.

As results, because of the large value of charge transferred to the fullerene cages, the HOMO–LUMO gap energy is decreased (see Fig. 13) which leads to high reactivity of $\text{Ng}_n\text{@C}_{80}$ and $\text{Ng}_n\text{@Si}_{80}$ structures. In conclusion, our calculations illustrated that, in general, the reactivity of $\text{Ng}_n\text{@C}_{80}$ and $\text{Ng}_n\text{@Si}_{80}$ structures is increased when the curvature in the fullerene cage is increased.

4. Conclusions

In this work, encapsulation of helium, neon and argon atoms into C_{80} and Si_{80} fullerene nanocage has been explored through DFT calculations. The stabilization energy, cavity volume, internal gas pressure as well as energy gap as a function of n (number of noble gas atoms) is investigated. The stabilization energy of the $\text{Ng}_n\text{@C}_{80}$ structures is increased by increasing the number of noble gas atoms

which means that these structures are metastable. Furthermore, although some of these structures are highly endothermic and they are unlikely to be formed, they still correspond to the local minima of potential energy surface. It is found that for low density of noble gas atoms, the stabilization energy of $\text{Ng}_n@\text{Si}_{80}$ structures is gradually decreased as n increases. For large number of n , the stabilization energy is increased by increasing n . In other words, for low density of noble gas atoms encapsulated inside Si_{80} , the $\text{Ne}_n@\text{Si}_{80}$ structures are truly energetically favorable and more stable than the $\text{Ne}_n@\text{C}_{80}$ structures. Results have shown that the maximum number of helium, neon and argon atoms which trapped into C_{80} , and formed a metastable structure, is determined to be $n = 46, 24$ and 10 respectively. The helium atom content of $\text{He}_{46}@\text{C}_{80}$ is approximately 19.16% . On the other hand, the maximum capacity of Si_{80} for helium, neon and argon gas atoms is found to be $95, 56$ and 22 atoms respectively. From the mechanism of $\text{He}_{50}@\text{C}_{80}$ breaking it is found that the final optimization of $\text{He}_{50}@\text{C}_{80}$ structure is very remarkable; this structure is similar to shopping cart; therefore, we named this structure as *Molecular Cart*. In the case of $\text{Ar}_{19}@\text{Si}_{80}$, if a single Si atom attached into the inner surface of this structure, a new phenomena as *Molecular Cesarean Section* is occurred. Results showed that the encapsulated noble gas atoms are a wide variety of molecular clusters. Finally, the dependence cage volume, internal gas pressure, charge transferred to the fullerene cage and energy gap of $\text{Ng}_n@\text{C}_{80}$ and $\text{Ng}_n@\text{Si}_{80}$ structures on n are also considered. The cage volume of $\text{Ng}_n@\text{C}_{80}$ and $\text{Ng}_n@\text{Si}_{80}$ structures are increased by increasing the number of encapsulated gas atoms due to elongation of fullerene C–C and Si–Si bonds. The calculated charge distribution show that the significant charge transfer from Ng clusters to fullerene cage is occurred. In conclusion, our calculations illustrated that, in general, the reactivity of $\text{Ng}_n@\text{C}_{80}$ and $\text{Ng}_n@\text{Si}_{80}$ structures is increased when the curvature in the fullerene cage is increased.

Acknowledgement

This work was supported by the Shahid Chamran University of Ahvaz – Iran for their supports in this scientific research.

Appendix A. Supplementary data

Supplementary data associated with this article can be found, in the online version, at <http://dx.doi.org/10.1016/j.jmgm.2014.08.006>.

References

- [1] H.W. Kroto, J.R. Heath, S.C.O. Brien, R.F. Curl, R.E. Smalley, C_{60} : buckminsterfullerene, *Nature* 318 (1985) 162–163.
- [2] J.R. Heath, S.C.O. Brien, Q. Zhang, Y. Liu, R.F. Curl, H.W. Kroto, F.K. Tittel, R.E. Smalley, Lanthanum complexes of spheroidal carbon shells, *J. Am. Chem. Soc.* 107 (1985) 7779–7780.
- [3] H. Jian, H. Yang, M. Yu, Z. Liu, C.M. Beavers, M.M. Olmstead, A.L. Balch, Single samarium atoms in large fullerene cages. Characterization of two isomers of $\text{Sm}@\text{C}-92$ and four isomers of $\text{Sm}@\text{C}-94$ with the X-ray crystallographic identification of $\text{Sm}@\text{C}-1(42)-\text{C}-92$, $\text{Sm}@\text{C}-s(24)-\text{C}-92$, and $\text{Sm}@\text{C}-3v(134)-\text{C}-94$, *J. Am. Chem. Soc.* 134 (2012) 10933–10941.
- [4] T. Akasaka, F. Wudl, S. Nagase (Eds.), *Chemistry of Nanocarbons*, John Wiley & Sons, Ltd, Singapore, 2010.
- [5] X. Lu, T. Akasaka, S. Nagase, Chemistry of endohedral metallofullerenes: the role of metals, *Chem. Commun.* 47 (2011) 5942–5957.
- [6] M.C. Qian, S.N. Khanna, An ab initio investigation on the endohedral metallofullerene, *J. Appl. Phys.* 101 (2007), 09E1051–09E1053.
- [7] M.N. Chaur, F. Melin, A.L. Ortiz, L. Echegoyen, Chemical, electrochemical, and structural properties of endohedral metallofullerenes, *Angew. Chem. Int. Ed.* 48 (2009) 7514–7538.
- [8] Y. Rubin, T. Jarroson, G.W. Wang, M.D. Bartberger, K.N. Houk, G. Schick, K. Saunders, R.J. Cross, Insertion of helium and molecular hydrogen through the orifice of an open fullerene, *Angew. Chem.* 113 (2001) 1591–1594.
- [9] L. Pang, F. Brisse, Endohedral energies and translation of fullerene noble gas clusters G at C_n (G=He, Ne, Ar, Kr, and Xr – n=60 and 70), *J. Phys. Chem.* 97 (1993) 8562–8563.
- [10] M.S. Syamala, R.J. Cross, M. Saunders, Xe-129 NMR spectrum of xenon inside C_{60} , *J. Am. Chem. Soc.* 124 (2002) 6216–6219.
- [11] M. Saunders, H.A. Jimenez-Vazquez, R.J. Cross, R.J. Poreda, Stable compounds of helium and neon–He-at-the-cost-of- C_{60} and Ne-at-the-cost-of- C_{60} , *Science* 259 (1993) 1428–1430.
- [12] M. Saunders, H.A. Jimenez-Vazquez, R.J. Cross, S. Mroczkowski, M.L. Gross, D.E. Giblin, R.J. Poreda, Incorporation of helium, neon, argon, krypton, and xenon into fullerenes using high-pressure, *J. Am. Chem. Soc.* 116 (1994) 2193–2194.
- [13] M. Saunders, R.J. Cross, H.A. Jimenez-Vazquez, R. Shimishi, A. Khong, Noble gas atoms inside fullerenes, *Science* 271 (1996) 1693–1697.
- [14] M. Alvarez, E.G. Gillan, K. Holczer, R. Kaner, K.S. Min, R.L. Whetten, Lanthanum carbide (La_2C_{80}): a soluble dimetallofullerene, *J. Phys. Chem.* 95 (1991) 10561–10563.
- [15] T. Akasaka, S. Nagase, K. Kobayashi, M. Walchli, K. Yamamoto, H. Funasaka, M. Kako, T. Hoshino, T. Erata, C-13 and La-139 NMR studies of $\text{La}_2@\text{C}_{80}$: first evidence for circular motion of metal atoms in endohedral dimetallofullerenes, *Angew. Chem.* 109 (1997) 1716–1719.
- [16] A. Rodriguez-Fortea, A.L. Balch, J.M. Poblet, Endohedral metallofullerenes: a unique host-guest association, *Chem. Soc. Rev.* 40 (2011) 3551–3563.
- [17] A. Rodriguez-Fortea, N. Alegret, A.L. Balch, J.M. Poblet, The maximum pentagon separation rule provides a guideline for the structures of endohedral metallofullerenes, *Nat. Chem.* 2 (2010) 955–961.
- [18] N. Alegret, M. Mulet-Gas, X. Aparicio-Angles, A. Rodriguez-Fortea, J.M. Poblet, Electronic structure of IPR and non-IPR endohedral metallofullerenes: connecting orbital and topological rules, *C. R. Chim.* 15 (2012) 142–158.
- [19] M.D. Shultz, J.C. Duchamp, J.D. Wilson, C.Y. Shu, J. Ge, J. Zhang, H.W. Gibson, H.L. Fillmore, J.I. Hirsch, H.C. Dorn, P.P. Fatouros, Encapsulation of a radiolabeled cluster inside a fullerene cage, $(177)\text{Lu}(x)\text{Lu}((3-x))\text{N}@C(80)$: an interleukin-13-conjugated radiolabeled metallofullerene platform, *J. Am. Chem. Soc.* 132 (2010) 4980–4981.
- [20] M.D. Shultz, J.D. Wilson, C.E. Fuller, J. Zhang, H.C. Dorn, P.P. Fatouros, Metallofullerene-based nanoplatform for brain tumor brachytherapy and longitudinal imaging in a murine orthotopic xenograft model 1, *Radiology* 261 (2011) 136–143.
- [21] A. Khong, H.A. Jimenez-Vazquez, M. Saunders, R.J. Cross, J. Laskin, T. Peres, C. Lifshitz, R. Strongin, A.B. Smith, An NMR study of He_2 inside C_{70} , *J. Am. Chem. Soc.* 120 (1998) 6380–6383.
- [22] M. Bortz, M. Jansen, $\text{Ag}_{25}\text{Bi}_3\text{O}_{18}$, a potentially valence-unstable BiIII/BiV compound, *Angew. Chem. Int. Ed. Engl.* 30 (1991) 884–886.
- [23] X.Y. Ren, C.Y. Jiang, J. Wang, Z.Y. Liu, Endohedral complex of fullerene C_{60} with tetrahedrane, $\text{C}_4\text{H}_4@\text{C}_{60}$, *J. Mol. Graphics Model.* 27 (2008) 558–562.
- [24] T.V. Tropin, N. Jargalan, M.V. Avdeev, O.A. Kyzyma, R.A. Eremin, D. Sangaa, V.L. Aksenenko, Kinetics of cluster growth in polar solutions of fullerene: experimental and theoretical study of C_{60}/NMP solution, *J. Mol. Liq.* 175 (2012) 4–11.
- [25] T. Sternfeld, R.E. Hoffmann, M. Saunders, R.J. Cross, M.S. Syamala, M. Rabinovitz, Two helium atoms inside fullerenes: probing the internal magnetic field in $\text{C}_{60}(6-)$ and $\text{C}_{70}(6-)$, *J. Am. Chem. Soc.* 124 (2002) 8786–8787.
- [26] A. Krapp, G. Frenking, Is this a chemical bond? A theoretical study of $\text{Ng}(2)@\text{C}_{60}$ ($\text{Ng}=\text{He}, \text{Ne}, \text{Ar}, \text{Kr}, \text{Xe}$), *Chem. Eur. J.* 13 (2007) 8256–8270.
- [27] R. Tonner, G. Frenking, M. Lein, P. Schwerdtfeger, Packed to the rafters: filling up C_{60} with rare gas atoms, *Chem. Phys. Chem.* 12 (2011) 2081–2084.
- [28] T. Weiske, J. Hrusak, D.K. Bohme, H. Schwarz, Endohedral fullerene-noble gas clusters formed with high-energy bimolecular reactions of C_x^{++} ($x=60, 70; n=1, 2, 3$), *Chem. Acta* 75 (1992) 79–82.
- [29] R.L. Murry, G.E. Scuseria, Theoretical evidence for a C_{60} “window” mechanism, *Science* 263 (1994) 791–793.
- [30] T. Ohtsuki, K. Ohno, K. Shiga, Y. Kawazoe, Y. Maruyama, K. Masumoto, Insertion of Xe and Kr atoms into C_{60} and C_{70} fullerenes and the formation of dimmers, *Phys. Rev. Lett.* 81 (1998) 967–970.
- [31] L. Becker, R.J. Poreda, T.E. Bunch, An extraterrestrial carbon carrier phase for noble gases, *PNAS* 97 (2000) 2979–2983.
- [32] K.M. Ho, A.A. Shvartsburg, B. Pan, Z.Y. Lu, C.Z. Wang, J.G. Wacker, J.L. Fye, M.F. Jarrold, Structures of medium-sized silicon clusters, *Nature* 392 (1998) 582–585.
- [33] M. Ohara, K. Miyajima, A. Pramann, A. Nakajima, K. Kaya, Geometric, Electronic structures of terbium–silicon mixed clusters (TbSi_n ; $6 \leq n \leq 16$), *J. Phys. Chem. A* 106 (2002) 3702–3705.
- [34] M. Ohara, K. Koyasu, A. Nakajima, K. Kaya, Geometric and electronic structures of metal (M)-doped silicon clusters (M=Ti, Hf, Mo and W), *Chem. Phys. Lett.* 371 (2003) 490–497.
- [35] K. Koyasu, M. Akutsu, M. Mitsui, A. Nakajima, Selective formation of MSi_{16} ($\text{M}=\text{Sc}, \text{Ti}$, and V), *J. Am. Chem. Soc.* 127 (2005) 4998–4999.
- [36] X.G. Gong, Q.Q. Zheng, Electronic structures and stability of Si_{60} and $\text{C}_{60}@\text{Si}_{60}$ clusters, *Phys. Rev. B* 52 (1995) 4756–4759.
- [37] H. Hiura, T. Miyazaki, T. Kanayama, Formation of metal-encapsulating Si cage clusters, *Phys. Rev. Lett.* 86 (2001) 1733–1736.
- [38] J. Li, J. Wang, H.Y. Zhao, Y. Liu, Role of encapsulated europium atoms, *J. Phys. Chem. C* 117 (2013) 10764–10769.
- [39] S.M. Beck, Studies of silicon cluster–metal atom compound formation in a supersonic molecular beam, *J. Chem. Phys.* 87 (1987) 4233–4234.
- [40] W. Ma, F. Chen, Electronic, magnetic and optical properties of Cu, Ag, Au-doped Si clusters, *J. Mol. Model.* 19 (2013) 4555–4560.
- [41] J. Wang, Y. Liu, Y.C. Li, Magnetic silicon fullerene, *Phys. Chem. Chem. Phys.* 12 (2010) 11428–11431.

- [42] J.P. Perdew, K. Burke, M. Ernzerhof, Generalized gradient approximation made simple, *Phys. Rev. B* 77 (1996) 3865–3868.
- [43] C.J. Cramer, *Essentials of Computational Chemistry: Theories and Models*, John Wiley & Sons Ltd, Barcelona Supercomputing Center, 2002.
- [44] P. Ordejan, E. Artacho, J.M. Soler, Self-consistent order-N density-functional calculations for very large systems, *Phys. Rev. B* 53 (1996) 10441–10444.
- [45] J.M. Soler, E. Artacho, J.D. Gale, A. García, J. Junquera, P. Ordejan, D. Sanchez-Portal, The SIESTA method for ab initio order-N materials simulation, *J. Phys. Condens. Matter* 14 (2002) 2745–2729.
- [46] <http://www.uam.es/siesta/website>
- [47] M.J. Frisch, et al., Gaussian03, Revision B.03, Gaussian, Inc., Pittsburgh, PA, 2003.
- [48] O.V. Pupysheva, A.A. Farajian, B.I. Yakobson, Fullerene nanocage capacity for hydrogen storage, *Nano Lett.* 8 (2008) 767–774.
- [49] L.J. Guo, X. Liu, G.F. Zhao, Y.H. Luo, Computational investigation of TiSi_n ($n=2$ –15) clusters by the density-functional theory, *J. Chem. Phys.* 126 (2007) 234704–234707.
- [50] S. Barman, P. Sen, G.P. Das, Ti-decorated doped silicon fullerene: a possible hydrogen-storage material, *J. Phys. Chem. C* 112 (2008) 19963–19968.
- [51] J.G. Han, Z.Y. Ren, L.S. Sheng, Y.W. Zhang, J.A. Morales, F. Hagelberg, The formation of new silicon cages: a semiempirical theoretical investigation, *J. Mol. Struct.* 625 (2003) 47–58.
- [52] H. Dodziuk, Reply to the 'Comment on 'Modeling complexes of H-2 molecules in fullerenes' by H. Dodziuk [Chem. Phys. Lett. 410 (2005) 39]' by L. Turker and S. Erkoc, *Chem. Phys. Lett.* 426 (2006) 224–225.
- [53] H. Dodziuk, Modeling the structure of fullerenes and their endohedral complexes involving small molecules with nontrivial topological properties, *J. Nanosci. Nanotechnol.* 7 (2007) 1102–1110.
- [54] R.E. Barajas-Barraza, R.A. Guirado-Lopez, Clustering of H-2 molecules encapsulated in fullerene structures, *Phys. Rev. B* 66 (2002) 155426–155437.
- [55] A. Bil, C.A. Morrison, Modifying the fullerene surface using endohedral noble gas atoms: density functional theory based molecular dynamics study of C₇₀O₃, *J. Phys. Chem. A* 116 (2012) 3413–3419.
- [56] S. Osuna, K.N. Houk, Cycloaddition reactions of butadiene and 1,3-dipoles to curved arenes, fullerenes, and nanotubes: theoretical evaluation of the role of distortion energies on activation barriers, *Chem. Eur. J.* 15 (2009) 13219–13231.
- [57] M. Garcia-Borras, S. Osuna, J.M. Luis, M. Swart, M. Sola, A complete guide on the influence of metal clusters in the Diels–Alder regioselectivity of Ih-C₈₀ endohedral metallofullerenes, *Chem. Eur. J.* 19 (2013) 14931–14940.
- [58] S. Osuna, M. Swart, M. Sola, Reactivity and regioselectivity of noble gas endohedral fullerenes Ng@C₆₀ and Ng₂@C₆₀ (Ng = He–Xe), *Chem. Eur. J.* 15 (2009) 13111–13123.